Proceedings of Czech–Japanese Seminar in Applied Mathematics 2004
August 4-7, 2004, Czech Technical University in Prague
http://geraldine.fjfi.cvut.cz
pp. 195–206

FULLY TWO DIMENSIONAL HLLEC RIEMANN SOLVER

PAVEL VÁCHAL[1] , RICHARD LISKA[1] , AND BURTON WENDROFF[2]

Abstract. Fully two dimensional sixteen state HLLEC (Harten, Lax, van Leer, Einfeldt, with contact correction) approximate Riemann solver has been developed for hydrodynamical Euler equations. The solver is applied to first order Godunov and second order WAF (Weighted Average Flux) finite difference schemes. The results yield improved treatment of contact discontinuities, stationary contacts are resolved exactly.

Key words. Euler equations, approximate Riemann solver, conservation laws

AMS subject classifications. 35L65, 65M06, 76N15

1. Introduction. The aim of this paper is to study the class of HLLE approximate Riemann solvers for Euler equations of gas dynamics and suggest a fully two dimensional extension of the one dimensional HLLC Riemann solver from [7]. We will be concerned with the family of HLLE approximate Riemann solvers. The first three characters in this name stand for Harten, Lax and van Leer, who suggested [3] to approximate the solution of the Riemann problem by three constant states, separated by two waves, propagating with constant speeds. Particular algorithms for computation of these wave speeds were presented five years later by Davis [1] and Einfeldt [2]. Here, we will follow Einfeldt's implementation. This explains the last character in the abbreviation HLLE. Then, the evolution continued in two directions. Since the assumption of two waves is correct only for hyperbolic systems of two equations, Toro, Spruce and Speares [7] added one more wave, creating so the 4-state one dimensional HLLC solver. In fluid dynamics, this new wave corresponds to a contact discontinuity. And really, the HLLC solver resolves contact discontinuities much better than his predecessor, the stationary ones even exactly. Later, Wendroff presented a series of 9-state solvers, extending the 3-state HLLE approach to two dimensions [11], [10]. Due to doubts about efficiency, he decided not to construct a straightforward extension of the contact-corrected 4-state HLLC solver. Here, we follow the path abandoned by Wendroff and extend the contact-corrected approach to a fully two dimensional 16-state HLLEC approximate Riemann solver. A brief description of this solver together with its usage in Godunov and WAF schemes has been presented in [9]. Here the full derivation of the approximate Riemann solver is presented.

2. One Dimensional HLLE and HLLEC Riemann Solvers. Methods presented in this paper have been derived for Euler equations

$$\begin{pmatrix} \rho \\ \rho u \\ \rho v \\ E \end{pmatrix}_t + \begin{pmatrix} \rho u \\ \rho u^2 + p \\ \rho uv \\ (E+p)u \end{pmatrix}_x + \begin{pmatrix} \rho v \\ \rho uv \\ \rho v^2 + p \\ (E+p)v \end{pmatrix}_y = \vec{0}, \tag{2.1}$$

[1]Department of Physical Electronics, Faculty of Nuclear Sciences and Physical Engineering, Czech Technical University in Prague, Trojanova 13, 120 00 Prague, Czech Republic.
[2]Group T7, Los Alamos National Laboratory, Los Alamos, USA

where ρ is the density, (u, v) fluid velocity, p pressure and E the density of the total energy. Completing the system (2.1) by the equation of state for an ideal polytropic gas $p = (\gamma - 1)\left(E - 1/2\rho u^2\right)$, we can write it in 1D (by removing third equation and y flux) in the general differential form $\vec{w}_t + \vec{f}(\vec{w})_x = \vec{0}$.

Let us discretize the x-t-plane by a rectangular grid with cell centers $x_i = i\Delta x$, $i \in \{0, \pm 1, \pm 2, \ldots\}$, cell endpoints $x_{i+1/2} = (i + 1/2)\,\Delta x$ and discrete time levels $t_n = t_{n-1} + \Delta t(n)$. Further, we will also use the staggered mesh, with cells of the same size, but shifted by $\Delta x/2$ with respect to the original ones.

2.1. 1D 3-state HLLE Solver. Let's have the initial Riemann problem

$$w(x, t_1) = \begin{cases} W_0 & \text{for} \quad x_i \le x < x_{i+1/2} \\ W_1 & \text{for} \quad x_{i+1/2} < x \le x_{i+1} \end{cases}. \tag{2.2}$$

Following [10], we approximate the solution at $t_1 < t < t_1 + \Delta t$ with three constant states W_0, W^* and W_1, divided by two waves, propagating with constant speeds b^0 and b^1. The situation is shown in Fig. 2.1(a). With this layout, the integral form

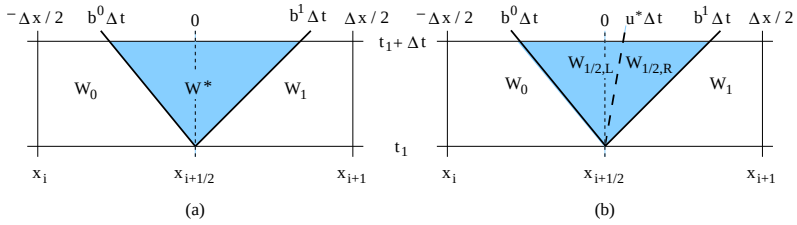

FIG. 2.1. *1D 3-state solver (a) and 4-state solver (b)*

of the 1D version of (2.1) integrated over staggered cell from x_i to x_{i+1} in space and from t_1 to $t_1 + \Delta t$ in time becomes

$$\begin{aligned} \frac{\Delta x}{2}(W_0 + W_1) = &\left(\frac{\Delta x}{2} + b^0\Delta t\right) W_0 + \left(b^1\Delta t - b^0\Delta t\right) W^* + \\ &+ \left(\frac{\Delta x}{2} - b^1\Delta t\right) W_1 + \left[f(W_1) - f(W_0)\right]\Delta t. \end{aligned} \tag{2.3}$$

Note, that data below the plots in Fig. 2.1 show the absolute position, while data above the plots are relative distances to the center of the staggered cell.

Resolving (2.3) with respect to W^* gives the central state value

$$W^* = \frac{b^1 W_1 - b^0 W_0 - f(W_1) + f(W_0)}{b^1 - b^0}. \tag{2.4}$$

To have the scheme totally determined, we must decide, how to choose wave speeds b^0 and b^1. We again follow [10] and use the Einfeldt speeds [2], based on Roe averages.

2.2. 1D 4-state HLLEC-based Solver. The 3-state HLLE Riemann solver, presented above, consists of two waves, dividing the staggered cell into three regions with constant states. As mentioned above, Toro et al. [7] extended it to a 4-state version, called HLLC, which resolves contact discontinuities better. The main idea is to split the intermediate state by the third wave, representing a contact, shown in Fig. 2.1(b). Since the velocity and pressure stay constant across contact discontinuities, the two central states differ only in density.For the initial Riemann problem

(2.2) with $W_0 = (\rho_0, \rho_0 u_0, E_0)^T$ $W_1 = (\rho_1, \rho_1 u_1, E_1)^T$ we compute the intermediate state from (2.4) the same way as in the 3-state solver and denote this state by $W^* = (\rho^*, \rho^* u^*, E^*)^T$. We assume u^* and p^* to be preserved across the central wave which moves with speed u^* as a contact discontinuity. The densities in the two new intermediate regions can be computed from the scalar Rankine-Hugoniot condition for the mass conservation, applied to the left, resp. right wave:

$$\rho_{1/2,L} = \rho^* \frac{u_0 - b^0}{u^* - b^0} \quad , \quad \rho_{1/2,R} = \rho^* \frac{u_1 - b^1}{u^* - b^1}. \tag{2.5}$$

3. Two Dimensional Solvers. First, we describe the fully two dimensional 9-state HLLE Riemann solver, originally presented in [10]. In this first implementation, wave speeds have been restricted by certain unnecessary conditions, which have been removed in [8]. Here, we introduce the latter version. Then we demonstrate its step-by-step transformation into a new 16-state HLLEC solver, which principally resolves also contact discontinuities. So, let us again start with the discretization.

We subdivide the x-y plane by a rectangular grid with cell centers at $(x_i, x_j) = (i\Delta x, j\Delta y)$, where $i, j \in \{0, \pm 1, \pm 2, \ldots\}$ and assume, that after each time step, the state variables are constant inside each cell. Then, in each corner $(x_{i+1/2}, y_{j+1/2}) = ((i + 1/2)\,\Delta x, (j + 1/2)\,\Delta y)$, we have an interface of four cells, forming a two dimensional Riemann problem. When we choose the time step small enough, these Riemann problems do not interfere with each other and we can solve each of them separately.

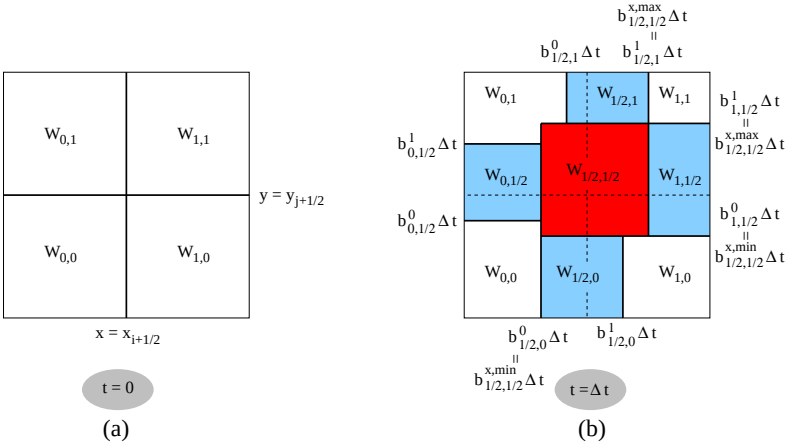

FIG. 3.1. *2D 9-state solver: the initial Riemann problem (a) evolves in time, splitting the staggered cell into 9 pieces (b).*

3.1. 2D 9-state HLLE Solver. The two dimensional Riemann problem at $\left(x_{i+1/2}, y_{j+1/2}\right)$, shown in Fig. 3.1(a), evolves in time and here we assume that it splits the staggered cell into 9 regions. An approximation of the status after some time interval Δt is shown in Fig. 3.1(b). The waves propagate from the center with constant speeds. For Δt sufficiently small, none of the waves in y-direction does reach the edge $y = y_j$, so that the state $W_{1/2,0}$ is affected only by the one dimensional Riemann problem in x-direction, given by $W_{0,0}$ and $W_{1,0}$. Analogous considerations along the other three edges lead us to following method: The corner states $(W_{0,0}, W_{1,0}, W_{0,1}, W_{1,1})$ stay undisturbed. We take them to compute the edge states $\left(W_{1/2,0}, W_{1/2,1}, W_{0,1/2}, W_{1,1/2}\right)$, using a 3-state solver based on the 1D HLLE

solver from section 2.1. Then we do not need to solve the real two dimensional problem in the central area, since $W_{1/2,1/2}$ is given by a two dimensional conservation law, applied to the whole staggered cell.

It is not exactly correct to say, that we "use the 1D 3-state solver" along the edges. Now, we are in two dimensions, and so we have one more state variable, which must be conserved: the transversal momentum ρv. Furthermore, we have a new flux in $y-$direction, and all vectors have now four components. Fortunately, we can drop off some terms. Fig. 3.2 shows in detail the region along the lower edge ($y = y_j$),

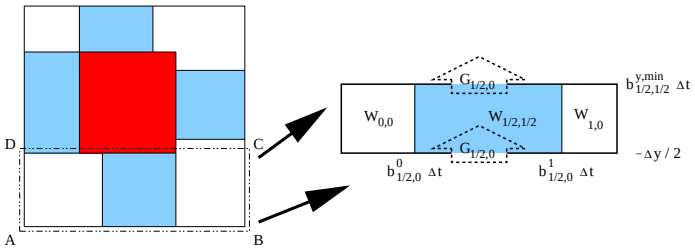

FIG. 3.2. *2D 9-state solver: Computing 1D problems along the edges with a 3-state solver. Fluxes in y-direction are the same and so they drop off.*

inside the rectangle $ABCD$. We want to compute the intermediate (blue) state $W_{1/2,0}$ so, that *two dimensional* integral conservation laws over the whole rectangle $ABCD$ hold. Since we have always only one state in $y-$direction, fluxes through the upper and lower border ($g-$fluxes) are the same and thus we can drop them off. Our system to solve is (2.1) without the y flux $(.)_y$. This is very similar to the one dimensional problem.So we can use the 3-state 1D solver (2.4) to compute the state $W_{1/2,0}$ but with the 1D fluxes changed to 2D $f-$fluxes according of (2.1), and inserting the transversal momentum ρv into the vector W of conserved variables. We perform the same operations along the upper edge of the staggered cell ($y = y_{j+1}$). Both 1D problems in $y-$direction, i.e. along edges $x = x_i$ and $x = x_{i+1}$ will be computed similarly, this time with $g-$fluxes and dropping the $f-$fluxes off.

The central red region in Fig. 3.1 is bordered by minimal and maximal wave speeds in x and y directions obtained from 1D Riemann problems along edges. Now, let us see, how to compute the central (red) state $W_{1/2,1/2}$. Applying the integral conservation law to the whole staggered cell centered at $\left(x_{i+1/2}, y_{j+1/2}\right) = \left((i+1/2)\,\Delta x, (j+1/2)\,\Delta y\right)$, we get (due to the simple geometry of an approximate Riemann solver with constant states)

$$\sum_{\alpha,\beta\in\{0,1/2,1\}} A_{\alpha,\beta} W_{\alpha,\beta} = \frac{\Delta x \Delta y}{4} \sum_{\gamma,\delta\in\{0,1\}} W_{\gamma,\delta} - \\ -\Delta t \Delta y \left(F_{1,1/2} - F_{0,1/2}\right) - \Delta t \Delta x \left(G_{1/2,1} - G_{1/2,0}\right) \tag{3.1}$$

where $W_{\alpha,\beta}$ represent the states, $A_{\alpha,\beta}$ the areas of regions occupied by these states at time Δt, and $F_{0,1/2}$, $F_{1,1/2}$ resp. $G_{1/2,0}$, $G_{1/2,1}$ the numerical fluxes through time-like faces of the staggered cell. These are

$$F_{0,1/2} = \frac{1}{2\Delta y}\Big[\left(\Delta y + b^0_{0,1/2}\Delta t\right) f\left(W_{0,0}\right) + \\ + \left(b^1_{0,1/2} - b^0_{0,1/2}\right)\Delta t f\left(W_{0,1/2}\right) + \left(\Delta y - b^1_{0,1/2}\Delta t\right) f\left(W_{0,1}\right)\Big] \tag{3.2}$$

through edge $x = x_i$, resp.

$$G_{1/2,0} = \frac{1}{2\Delta x}\Big[\Big(\Delta x + b^0_{1/2,0}\Delta t\Big)\, g\left(W_{0,0}\right) + \\ + \Big(b^1_{1/2,0} - b^0_{1/2,0}\Big)\, \Delta t g\left(W_{1/2,0}\right) + \Big(\Delta x - b^1_{1/2,0}\Delta t\Big)\, g\left(W_{1,0}\right)\Big] \tag{3.3}$$

through edge $y = y_j$, and similarly for the other two edges. Since we already know all other states, all areas, speeds, fluxes and constants, we can resolve (3.1) with respect to $W_{1/2,1/2}$ and compute the central state.

3.2. From 9-state HLLE to 16-state HLLEC. Our next objective is to develop a non-split, fully two dimensional HLLEC Riemann solver. Let us summarize our requirements:

- First, the solver should be (as much as possible) a straightforward extension of the one dimensional 4-state HLLEC solver from section 2.2. This means, in 2D we would have 16 states.
- Further we require, that it degenerates to the 1D solver for purely 1D problems in coordinate directions. In other words, if the initial condition is a Riemann problem with only one interface, for example $W_{UL} = W_{LL}$ and $W_{UR} = W_{LR}$, the solver has to consist of four stripes with constant states. Since we will have a 16-state solver, each of these stripes will be formally divided into four regions with identical states. Note, that this degeneracy should take place also in the case of nonzero transversal velocities, and even if these velocities differ in the initial left and right states. The same must of course hold also for the problem rotated by 90 degrees (Fig. 3.3(b)).

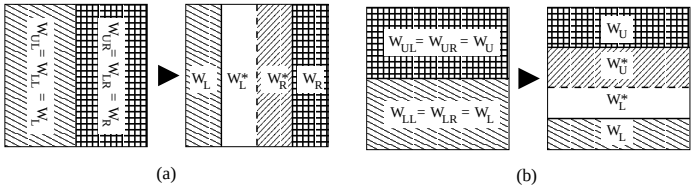

FIG. 3.3. *2D HLLC solver: Desired degeneracy to 1D 4-state solver for 1D initial problems along the coordinate directions.*

- Another property of the 1D HLLEC solver, which we want to retain also in 2D, is the exact resolution of stationary contact discontinuities in coordinate directions. This is very important, since contact discontinuities are the main motivation to construct HLLEC solvers.

3.2.1. Splitting the Peripheral Regions. The simplest extension of the 9-state solver is to split the intermediate region in each of the one dimensional problems along the edges. That means, we replace the 3-state HLLE solver from section 2.1 by the 4-state HLLEC from section 2.2. We are now in 2D and so, as in the 9-state approach, we must modify the 1D solvers to obey also 2D conservation laws. Let us again consider the region along the lower edge ($y = y_j$), i.e. the rectangle $ABCD$ from Fig. 3.2. The computation along other three edges of the staggered cell will be fully analogous.

We want to compute two intermediate (blue) states in Fig. 3.4(b) so, that *two dimensional* integral conservation laws over the whole rectangle are fulfilled. As in

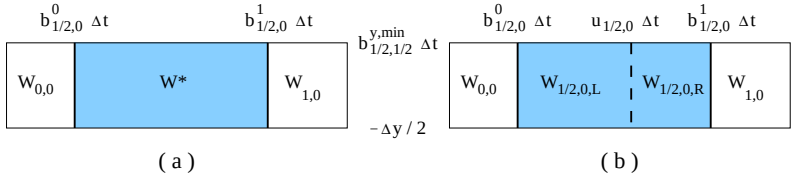

FIG. 3.4. *2D HLLEC solver: "One dimensional" strip along the lower edge (magnified part of Fig.3.2). Computing the intermediate state (a) and splitting it into two (b).*

the 9-state solver, the $g-$fluxes (through lower and upper border) are the same and so they drop out, which means that we again have to solve the pseudo-1D system.

First, we compute the whole, unsplit central state, denoted by W^* in Fig. 3.4(a) with a 3-state solver (2.4). Then, exactly as we did in the 1D 4-state HLLEC solver, we split the intermediate region by a wave approximating a contact discontinuity. The longitudinal velocity is preserved across the contact, thus we set $u_{1/2,0,L} = u_{1/2,0,R} = u_{1/2,0}$. Densities $\rho_{1/2,0,L}$ and $\rho_{1/2,0,R}$ can again be computed from the Rankine-Hugoniot condition for mass conservation, applied to the left, resp. right wave (2.5). Transversal velocity is advected with the contact, so we set $v_{1/2,0,L} = v_{0,0}$ and $v_{1/2,0,R} = v_{1,0}$. Finally, we compute the central pressure from the total energy conservation

$$(3.4)\qquad \left(u_{1/2,0} - b^0_{1/2,0}\right) E_{1/2,0,L} + \left(b^1_{1/2,0} - u_{1/2,0}\right) E_{1/2,0,R} = \left(b^1_{1/2,0} - b^0_{1/2,0}\right) E^*.$$

Since pressure is constant across contact discontinuities, we assume it to be equal for both intermediate states.

By such splitting of intermediate (blue) regions along all four edges, we obtain a 13-state solver shown in Fig. 3.5(a). Now, we have to compute the central red state $W_{1/2,1/2}$.

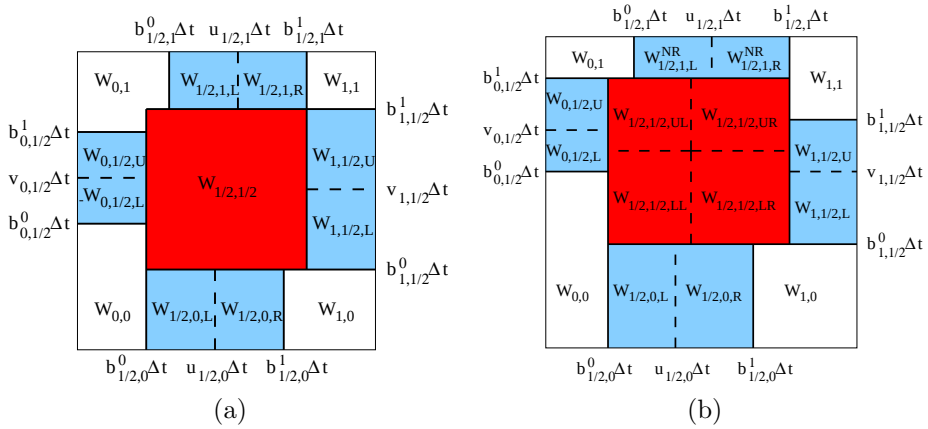

FIG. 3.5. *2D 13-state solver (a) and 2D 16-state solver(b).*

3.2.2. Computing the 13th State. Up to now, our solver consists of 13 regions (see Fig. 3.5(a)): four in the corners (white), eight along the edges (blue) and one (the 13th) in the center (red). First, we compute the areas of all these regions. Let us denote them A_σ, where σ indicates the state. Now we apply the two dimensional

integral conservation law in the same way as we did in the 9-state solver (3.1), but now taking into account also the splitting of (blue) edge states:

$$
\begin{aligned}
A_{1/2,1/2}W_{1/2,1/2} = & \sum_{\alpha,\beta\in\{0,1\}} \left(\frac{\Delta x\Delta y}{4} - A_{\alpha,\beta}\right) W_{\alpha,\beta} - \\
& - \sum_{\alpha\in\{0,1\}} \left(A_{\alpha,1/2,L}W_{\alpha,1/2,L} + A_{\alpha,1/2,U}W_{\alpha,1/2,U}\right) - \\
& - \sum_{\beta\in\{0,1\}} \left(A_{1/2,\beta,L}W_{1/2,\beta,L} + A_{1/2,\beta,R}W_{1/2,\beta,R}\right) - \\
& - \Delta t\Delta y \left(F_{1,1/2} - F_{0,1/2}\right) - \Delta t\Delta x \left(G_{1/2,1} - G_{1/2,0}\right),
\end{aligned} \tag{3.5}
$$

where the numerical fluxes through left and lower edges are

$$
\begin{aligned}
F_{0,1/2} = \frac{1}{2\Delta y} & \left[\left(\Delta y + b^0_{0,1/2}\Delta t\right) f\left(W_{0,0}\right) + \left(v_{0,1/2} - b^0_{0,1/2}\right)\Delta t\ f\left(W_{0,1/2,L}\right) + \right. \\
& \left. + \left(b^1_{0,1/2} - v_{0,1/2}\right)\Delta t\ f\left(W_{0,1/2,U}\right) + \left(\Delta y - b^1_{0,1/2}\Delta t\right) f\left(W_{0,1}\right)\right] \\
G_{1/2,0} = \frac{1}{2\Delta x} & \left[\left(\Delta x + b^0_{1/2,0}\Delta t\right) g\left(W_{0,0}\right) + \left(u_{1/2,0} - b^0_{1/2,0}\right)\Delta t\ g\left(W_{1/2,0,L}\right) + \right. \\
& \left. + \left(b^1_{1/2,0} - u_{1/2,0}\right)\Delta t\ g\left(W_{1/2,0,R}\right) + \left(\Delta x - b^1_{1/2,0}\Delta t\right) g\left(W_{1,0}\right)\right]
\end{aligned}
$$

and through the upper and right edges analogously. If there was only one state in the center (red), it would have the density $\rho_{1/2,1/2}$, the velocities $u_{1/2,1/2}$, $v_{1/2,1/2}$ and the total energy $E_{1/2,1/2}$ computed from (3.5). Such 13-state Riemann solver performs slightly better than the 9-state version, but does not degenerate to the 1D 4-state HLLEC solver for 1D initial conditions. We have to split the central region into four parts by two additional waves parallel to coordinate axes.

3.2.3. Splitting the Central Region. As in the 1D case, we can estimate the speeds of the splitting waves by the $x-$, resp. $y-$components of fluid velocity in the central region (i.e. the velocity of the 13th state). Unfortunately, we can no longer assume, that these waves are contact discontinuities having longitudinal velocities on both sides of contact equal to the speed of the contact wave. Under that assumption, velocities in all four central regions would have to be equal. Such solver could correctly degenerate to 1D in density, but not in momenta for the 1D problem with different transversal velocities. However, we can still assume, that pressure stays unchanged across these two splitting waves, i.e. that it is constant inside the whole central region.

We can use other speeds of splitting waves, for example the averages of contact speeds along the opposite cell edges (i.e. those splitting the blue regions). That is, if we use the notation as in Fig. 3.5(b) and report to the speeds of central splitting waves as to $u_{1/2,1/2}$ and $v_{1/2,1/2}$, we can take $u_{1/2,1/2} = (u_{1/2,0} + u_{1/2,1})/2$, $v_{1/2,1/2} = (v_{0,1/2} + v_{1,1/2})/2$. As can be clearly seen in Fig. 3.5(b), we require, that both splitting waves stay inside the central region (delimited by $b^{x,min}_{1/2,1/2}$, $b^{x,max}_{1/2,1/2}$, $b^{y,min}_{1/2,1/2}$ and $b^{y,max}_{1/2,1/2}$). The first approach described above (speeds = velocities of the 13th state) satisfies this condition for most usual problems. However, in some extreme cases, the splitting waves with such speeds would leave the central region. In such case we use the averages which work always. Beside these two, there are many other ways to split the central region.

Now, we need to compute states in the four central regions $W_{1/2,1/2,UL}$, $W_{1/2,1/2,UR}$, $W_{1/2,1/2,LL}$ and $W_{1/2,1/2,LR}$, shown in Fig. 3.5(b). First, we estimate the velocities and densities so, that our solver degenerates correctly to 1D as explained above. Then we correct these estimates to obey the mass and both momentum conservation laws. Finally, we set the value of the only remaining variable - the constant pressure, common for all four central states - so, that total energy is conserved. Let us study these steps in more detail.

3.2.4. Estimating Central Velocities. We need to estimate eight central velocities $u_{1/2,1/2,\alpha}, v_{1/2,1/2,\alpha}, \alpha \in \{UL, UR, LL, LR\}$. Constructing previous versions of our solver, we first tried to base these estimates directly on values of momenta in the 13th (red) state, which we obtained from the 2D conservation law. This was not correct, since such approach introduces the 2D element and does not degenerate properly to 1D.

Let us repeat, what exactly does degeneracy in momenta mean[1]. If the initial conditions form an one dimensional problem in x-direction (i.e. if $W_{UL} = W_{LL}$ and $W_{UR} = W_{LR}$), we would like to obtain four "1D" states independent on the y-coordinate. Transversal velocities (here v) stay unchanged, their interface is advected with speed of the central contact wave. We estimate the $x-$velocities $u_{1/2,1/2,\alpha}$ from the already known states neighboring up, resp. down, weighted by lengths of interfaces of the particular central region (red) with corresponding edge regions (blue) and corner regions (white). Similarly, we estimate four central $y-$velocities $v_{1/2,1/2,\alpha}$ from the states neighboring to the left, resp. right. For lucidity, the estimating procedure is shown schematically in Fig. 3.6. These estimates are based on properties of longitudinal and transversal velocities across contact waves and correctly degenerate to 1D as required.

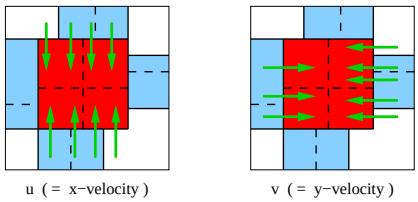

FIG. 3.6. *Estimating the central velocities in a way that preserves 1D degeneracy. Estimate for particular central region is based on values in states, where the corresponding arrows start.*

3.2.5. Estimating Central Densities. In the 1D problem along the edges (see section 3.2.1), we have computed intermediate densities from the Rankine-Hugoniot conditions for mass conservation law[2]. We will use these conditions also to estimate densities in four central (red) regions. At each segment of interface with surrounding (blue or white) states, we know the speed of splitting wave ($b^{x,min}_{1/2,1/2}$, $b^{x,max}_{1/2,1/2}$, $b^{y,min}_{1/2,1/2}$, or $b^{y,max}_{1/2,1/2}$), two velocities and one density. For each such segment, we compute the second density from the 1D Rankine-Hugoniot condition[2]. weigh the appropriate densities by lengths of these segments and get an average for each of the four central

[1]We will handle velocities here. The final scheme will be degenerative also in densities, so degeneracy will be achieved for momenta as well.

[2]Let us have two states W_A and W_B with constant densities ρ and velocities u, split by a simple wave, propagating with speed s. Then the condition in 1D is $\rho_A u_A - \rho_B u_B = s\,(\rho_A - \rho_B)$.

regions. These averages will be used as our estimations of central densities. The whole procedure for the upper right state is shown in Fig. 3.7. Densities $\rho^{(j)}$ in Fig. 3.7(b) are weight averaged by the lengths $d^{(j)}$. Other alternatives to this weighting are also possible [8].

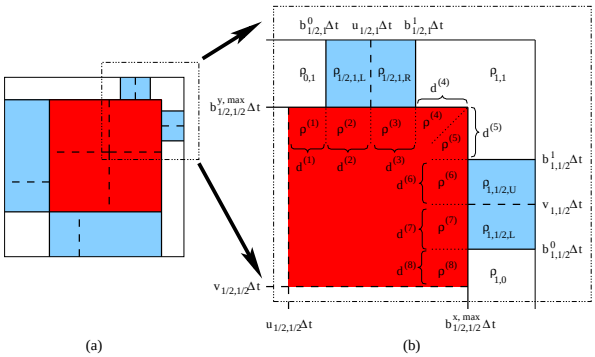

FIG. 3.7. *2D 16-state solver: Weighting the densities, resulting from 1D wave-propagation conditions, in order to get* $\rho_{1/2,1/2,UR}$. *(a) whole staggered cell, (b) magnified upper right part.*

3.2.6. Mass Conservation. To construct a conservative solver, we need that the total mass inside the whole central region remains the same as in case of the 13-state solver. Thus, central densities must obey

$$A_{1/2,1/2}\rho_{1/2,1/2} = A^{LL}_{1/2,1/2}\rho_{1/2,1/2,LL} + A^{LR}_{1/2,1/2}\rho_{1/2,1/2,LR} + A^{UL}_{1/2,1/2}\rho_{1/2,1/2,UL} + A^{UR}_{1/2,1/2}\rho_{1/2,1/2,UR}, \tag{3.6}$$

where $\rho_{1/2,1/2}$ is the 13th density, computed from the 2D mass conservation law, and A_σ are areas of appropriate regions. The estimates (weighted averages) from the previous step (section 3.2.5) have to be corrected to satisfy (3.6). One of many possibilities is to multiply each of them with an constant factor C:

$$\rho_{1/2,1/2,\alpha} = C\rho^{estim}_{1/2,1/2,\alpha} \quad , \quad \alpha \in \{UL, UR, LL, LR\} \tag{3.7}$$

where

$$C = \frac{A_{1/2,1/2}\rho_{1/2,1/2}}{A^{LL}_{1/2,1/2}\rho^{estim}_{1/2,1/2,LL} + A^{LR}_{1/2,1/2}\rho^{estim}_{1/2,1/2,LR} + A^{UL}_{1/2,1/2}\rho^{estim}_{1/2,1/2,UL} + A^{UR}_{1/2,1/2}\rho^{estim}_{1/2,1/2,UR}}. \tag{3.8}$$

This is possible, since all areas and all densities are positive. Another methods for correcting of the estimates are mentioned below (in section 3.2.7).

3.2.7. Conservation of Momenta. The conservation conditions for momenta are similar to (3.6), just with densities replaced by momenta:

$$A_{1/2,1/2}\rho_{1/2,1/2}u_{1/2,1/2} = \sum_{\alpha\in\{UL,UR,LL,LR\}} A^{\alpha}_{1/2,1/2}\rho_{1/2,1/2,\alpha}u_{1/2,1/2,\alpha}$$

$$A_{1/2,1/2}\rho_{1/2,1/2}v_{1/2,1/2} = \sum_{\alpha\in\{UL,UR,LL,LR\}} A^{\alpha}_{1/2,1/2}\rho_{1/2,1/2,\alpha}v_{1/2,1/2,\alpha}.$$

Unlike densities, velocities can be negative, and so the coefficient analogous to C from (3.8) could be also negative. Multiplying the momenta would then change their signs,

which would lead to fatal errors (for large velocities of similar magnitude in opposite directions). We have to find some other method to correct the velocities estimated in section 3.2.4.

In our implementation, we have chosen to *add* the same amount of momentum to each state. Then we have

$$\rho_{1/2,1/2,\alpha} u_{1/2,1/2,\alpha} = \rho_{1/2,1/2,\alpha} u^{estim}_{1/2,1/2,\alpha} + \Delta/4 \ , \ \alpha \in \{UL, UR, LL, LR\} \tag{3.9}$$

where

$$\Delta = \rho_{1/2,1/2} u_{1/2,1/2} - \frac{1}{A_{1/2,1/2}} \sum_{\alpha \in \{UL,UR,LL,LR\}} A^{\alpha}_{1/2,1/2} \rho_{1/2,1/2,\alpha} u_{1/2,1/2,\alpha} \tag{3.10}$$

and similarly for the y-momentum ρv. Note, that the correction by adding, analogous to (3.9), (3.10), could be used also earlier for density instead of multiplication (3.7), (3.8).

3.2.8. Energy Conservation and Central Pressure. We assume, that pressure is equal in all four central (red) states $p_{1/2,1/2} = p_{1/2,1/2,UL} = p_{1/2,1/2,UR} = p_{1/2,1/2,LL} = p_{1/2,1/2,LR}$. The central pressure is computed from conservation of the total energy

$$A_{1/2,1/2} E_{1/2,1/2} = \sum_{\alpha \in \{UL,UR,LL,LR\}} A^{\alpha}_{1/2,1/2} E_{1/2,1/2,\alpha}$$

which with the use of equation of state gives direct formula for $p_{1/2,1/2}$.

3.2.9. Degeneracy to 1D Solver for 1D Problems. Let us show, that our solver really degenerates as required in the beginning of section 3.2. Consider a 1D initial problem in x-direction. Since in this case $b^0_{1/2,0} = b^0_{1/2,1} = b^{x,min}_{1/2,1/2}$, $u_{1/2,0} = u_{1/2,1} = u_{1/2,1/2}$ and $b^1_{1/2,0} = b^1_{1/2,1} = b^{x,max}_{1/2,1/2}$, we have three continuous wavefronts in this direction, i.e. there are only three vertical partitions as shown in Fig. 3.3(a). Due to the initial condition, solutions of the 1D Riemann problems y-direction (left and right blue regions) are trivially equal to the adjacent corner states. Solution of both 1D Riemann problems in x-direction (upper and lower blue regions) are equal and the incoming and outgoing G-fluxes cancel each other. Thus, when checking for conservation, we only have to care about the F-fluxes. Since in this case the x-velocity estimates in the red regions are equal to values in corresponding blue regions neighboring up or down, the Rankine-Hugoniot condition across horizontal interfaces is trivial (no jump in anything). Now, the density estimates are given only by the jumps across the vertical interfaces and all values are the same as for the horizontal 1D Riemann problems. To summarize, the estimates of density and longitudinal velocity in the red states are equal to values in blue regions neighboring up or down and already these estimates satisfy the corresponding conservation laws. This is the same case also for pressure. We see, that in the case of 1D initial problem, no conservation correction in the red states is necessary and the solver really degenerates to 1D HLLEC. As for jumps in transversal velocity, the degeneracy requirement is still met, since everything happens along the continuous central wavefront.

4. Numerical results. In this section, we demonstrate, how approximate Riemann solvers can be used in difference schemes. The developed approximate Riemann solvers have been used in the first order Godunov and second order WAF [6] finite

difference schemes [9]. Here we present the results for one 2D Riemann problem (from a family presented at [5]) computed by these schemes. Computational domain $\langle 0,1\rangle \times \langle 0,1\rangle$ is split by two perpendicular lines, located at $x = 0.5$ and $y = 0.5$, into four quadrants, denoted UL (upper left), UR (upper right), LL (lower left) and LR (lower right). Each quadrant contains diatomic polytropic ideal gas ($\gamma = 1.4$), initially described by the constant values presented in Tab. 4.1. The initial data are chosen so that four 1D Riemann problems along the domain edges ($x = 0$, $x = 1$, $y = 0$ and $y = 1$) result in just one elementary wave, namely shock on right and up and contact on left and down as schematically shown in Tab. 4.1. Computations

$\rho_{UL} = 1.0$	$p_{UL} = 1.0$	$\rho_{UR} = 0.5313$	$p_{UR} = 0.4$
$u_{UL} = 0.7276$	$v_{UL} = 0$	$u_{UR} = 0$	$v_{UR} = 0$
$\rho_{LL} = 0.8$	$p_{LL} = 1.0$	$\rho_{LR} = 1.0$	$p_{LR} = 1.0$
$u_{LL} = 0$	$v_{LL} = 0$	$u_{LR} = 0$	$v_{LR} = 0.7276$

	S $\rightarrow$	
C		$\uparrow$ **S**
	C	

TABLE 4.1
Initial conditions for the test Riemann problem (test 12 from [4])

have been performed on a rectangular mesh of 400x400 cells, with $C_{CFL} = 0.49$ for both schemes. The results are shown in Fig. 4.1(a),(b),(c) for the Godunov scheme with 9-state and 16-state solver and for the WAF scheme with 16-state solver. Density is visualized by colors and by a set of equidistant contours. Clearly 9-state solver resolves badly the contact waves separating lower left quadrant. 16-state solver resolver stationary contacts exactly. The WAF scheme resolves better shock waves, both straight ones separating small blue region in the upper right corner and curved ones separating yellow-red central structure. This Riemann problem has two stationary contact discontinuities. To show resolution of moving contacts we present in Fig. 4.1(d) result of the WAF scheme with 16-state solver for similar Riemann problem with initial velocities shifted by (-0.2,-0.2) in all quadrants. Moving contact is resolved reasonably well. Also note a bubble-shaped formation in upper right corner of the lower left blue region. It is visible already in the Godunov scheme with 16-state solver (b), but resolved in much more detail by the WAF scheme (c),(d).This is in good correspondence with experiments on denser meshes as well as with other higher-order numerical schemes, however any proof of correct solution of 2D Riemann problems does not exist yet. As for the computational expenses, the ratio of CPU times in this particular test was 1.0 / 2.0 / 5.4 for results in Figs. 4.1(a)/(b)/(c).

5. Conclusion. We proposed a fully two dimensional extension of the one dimensional approximate Riemann solver from [7] and demonstrated its application in two particular difference schemes.

Acknowledgments. Partial support of the project No. 202/03/H162 of the Grant Agency of the Czech Republic, No. FRVS 2087/2004 of the Ministry of Education of the Czech Republic and No. CTU 0411014 of the Czech Technical University in Prague is acknowledged.

REFERENCES

[1] S. DAVIS, *Simplified second-order Godunov-type methods*, SIAM J. Sci. Stat. Comput., 9 (1988), pp. 445–473.
[2] B. EINFELDT, *On Godunov-type methods for gas dynamics*, SIAM J. Numer Anal., 25 (1988), pp. 294–318.

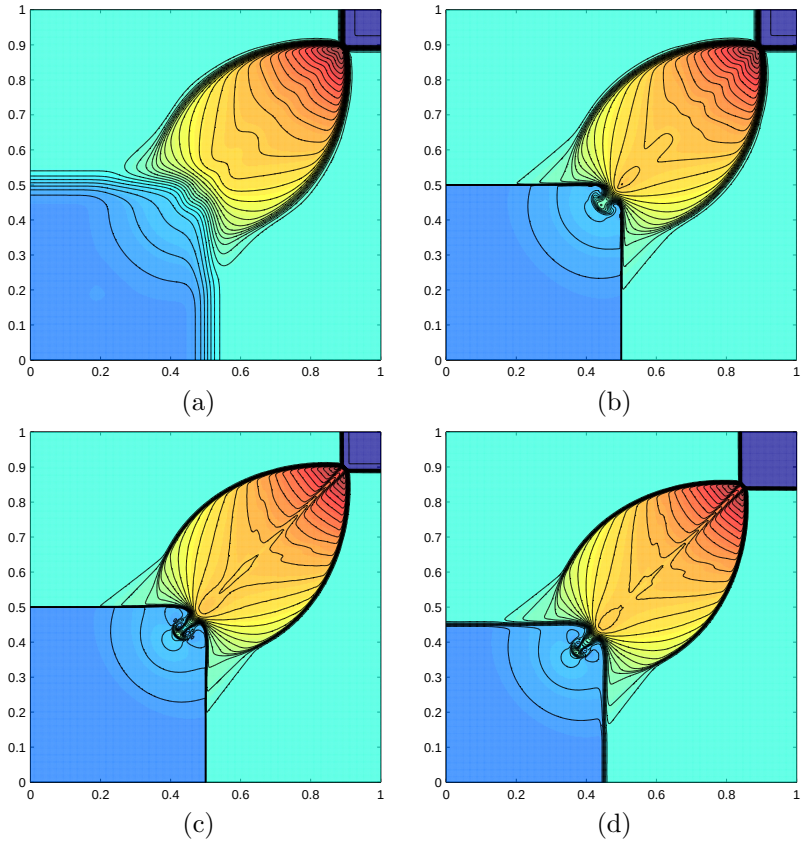

FIG. 4.1. *Density at time $t = 0.25$ units; color maps with 45 highlighted isolines computed by Godunov scheme with 9-state solver(a), by Godunov scheme with 16-state solver (b) and by WAF scheme with 16-state solver (c)(d); (a),(b),(c) are results of the Riemann problem defined in Tab. 4.1 with two stationary contacts while (d) is result for this problem with velocities shifted by (-0.2,-0.2).*

[3] A. HARTEN, P. LAX, AND B. VAN LEER, *On upstream differencing and Godunov-type schemes for hyperbolic conservation laws*, SIAM Rev., 25 (1983), pp. 35–61.
[4] P. D. LAX AND X.-D. LIU, *Solution of two dimensional Riemann problem of gas dynamics by positive schemes*, SIAM J. on Scientific Comp., 19 (1998), pp. 319–340.
[5] C. W. SCHULZ-RINNE, J. P. COLLINS, AND H. M. GLAZ, *Numerical solution of the Riemann problem for two-dimensional gas dynamics*, SIAM J. Sci. Comput., 14 (1993), pp. 1394–1414.
[6] E. TORO, *A weighted average flux method for hyperbolic conservation laws*, Proc. R. Soc. London A, 423 (1989), p. 401.
[7] E. TORO, M. SPRUCE, AND W. SPEARES, *Restoration of the contact surface in the HLL-Riemann solver*, Shock Waves, 4 (1994), pp. 25–34.
[8] P. VACHAL, *Some aspects of numerical resolution of contact discontinuities in conservation laws*, Master's thesis, Czech Technical University, 2003. (in English).
[9] P. VÁCHAL, R. LISKA, AND B. WENDROFF, *Fully two-dimensional HLLEC Riemann solver and associated difference schemes*, in Numerical Mathematics and Advanced Applications ENUMATH 2003, M. Feistauer, V. D. sí, P. Knobloch, and K. Najzar, eds., Berlin, 2004, Springer-Verlag, pp. 815–824.
[10] B. WENDROFF, *Approximate Riemann solvers, Godunov schemes, and contact discontinuities*, in Godunov Methods: Theory and Applications, E. Toro, ed., Oxford, UK, October 18-22, 1999, 1999.
[11] ———, *A two-dimensional HLLE Riemann solver and associated Godunov-type difference scheme for gas dynamics*, Computers and Math. with Applications, 38 (1999), pp. 175–185.